SAN ONOFRE NUCLEAR GENERATING STATION UNIT 1
LONG TERM SERVICE SEISMIC REEVALUATION PROGRAM

TECHNICAL BASIS FOR STRESS-STRAIN CORRELATION

Prepared for

NUCLEAR REGULATORY COMMISSION

Prepared by

SOUTHERN CALIFORNIA EDISON COMPANY

Report No. 01-0310-1459

October 7, 1985

TABLE OF CONTENTS

Section		Page
TABLE OF CONTENTS		1
1.0	INTRODUCTION	5
2.0	PIPING STRAIN CRITERIA	6
3.0	STRESS-STRAIN CORRELATION METHODOLOGY	8
4.0	JUSTIFICATION OF METHODOLOGY	8
4.1	ASME Code Fatigue Evaluation Procedure	10
4.2	Comparison with Greenstreet Elbow Test Results	18
5.0	APPLICATION LIMITATIONS	20
REFERENCES		21
APPENDIX A:	Comparison of Load-Strain Curves between Greenstreet Tests and SONGS-1 Stress-Strain Correlation Methodology	

1.0 INTRODUCTION

This document presents the piping strain criteria and stress-strain correlation methodology proposed for the piping qualification at San Onofre Nuclear Generating Station Unit 1 (SONGS-1) under the Long Term Service (LTS) Seismic Reevaluation Program. The purpose of this document is to present and justify the strain limit criteria and the stress-strain correlation methodology for use in the LTS piping qualification.

The criteria and methodology for the SONGS-1 LTS piping qualification have been discussed with the Nuclear Regulatory Commission (NRC) for the past few months. Based on the technical information presented for the SONGS-1 LTS work and on the NRC's technical comments, an overall approach is being developed for use on the project.

Figure 1-1 shows the overall piping analysis approach for SONGS-1 LTS piping qualification. Both linear and non-linear piping analysis techniques will be used. Linear piping analysis techniques include applications of enveloped response spectra method, multiple-level response spectra method, linear time-history analysis method and similarity method. In lieu of linear piping analysis techniques, non-linear analysis techniques may be used for some piping systems on a case-by-case basis. Nonlinear piping analysis techniques include applications of nonlinear time-history analysis method, energy balance method and secant stiffness method. For small bore piping and tubing, walkdown and chart method may also be used. Detailed descriptions of these analysis methods are presented in earlier submittals to the NRC [2,3] and in the NRC's Safety Evaluation Report for SONGS-1 LTS seismic reevaluation criteria and methodology [4].

When linear piping analysis techniques are used, the resulting piping stresses will be compared to the Systematic Evaluation Program (SEP) criteria; as shown below:

$$\sigma_e = \frac{PD_o}{4t} + 0.75\, i\, \frac{M_a + M_b}{Z} \leq kS_h$$

where

P = Maximum internal operating pressure, psig
D_o = Outside diameter of pipe, in
t = Nominal wall thickness of pipe, in
Z = Section modulus of pipe, in^3
i = Stress intensification factor as listed in Fig. NC-3673.2(b)-1 of ASME B&PV Code, Section III, Subsection NC, 1980 Edition, Winter 1980 Addenda [1].
M_a = Resultant moment due to gravity loads, in-lbs
M_b = Resultant moment due to Modified Housner Earthquake inertia, as calculated by linear elastic methods, in-lbs (Resultant moment due to Modified Housner Earthquake anchor movements may be combined

with inertia moments by Square-Root-of-the-Sum-of-the-Square (SRSS) method, if omitted in the secondary stress check as defined by ASME Code Class 2 piping Equations 10 and 11 in NC-3652.3[1]).

S_h = Piping material allowable stress at maximum operating temperature, psi (obtain S_h from Appendix I of the Code [1]).

k = 2.4 for Class 2 and 3 piping
= 1.8 for Class 1 piping

In cases where the elastically-calculated primary piping stresses exceed the SEP allowables, the primary stress σ_e, as defined above, may be correlated to a piping strain and then compared to an allowable strain. Figure 1-2 shows a flow chart for piping stress-strain correlation.

This document describes the conversion of the linear elastically-calculated stresses to strains. Section 2.0 presents the piping strain limits and Section 3.0 presents the stress-strain correlation methodology. Section 4.0 presents the justifications of the proposed methodology. Section 5.0 presents the application limitations.

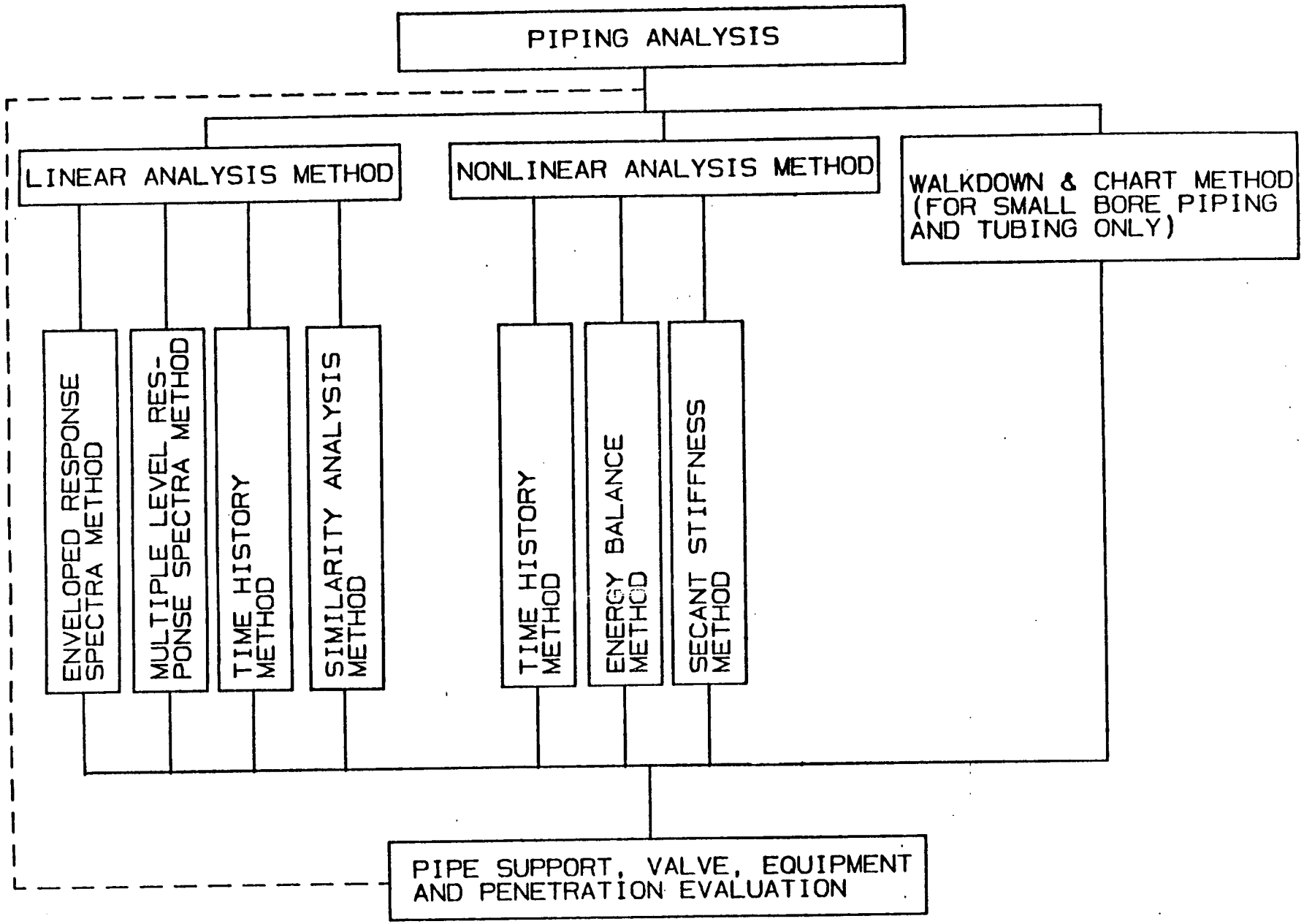

Figure 1-1: Overall Piping Analysis Approach

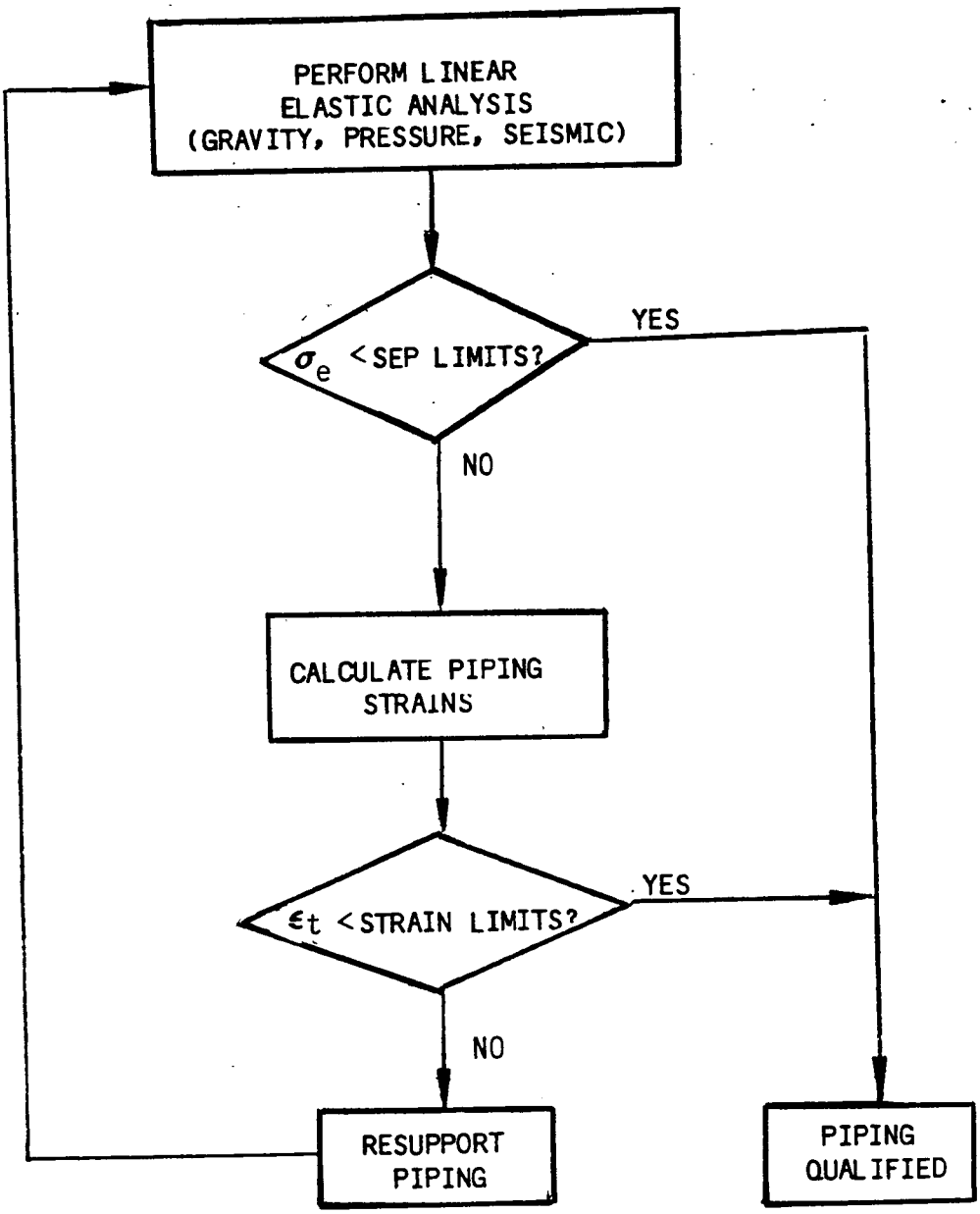

Figure 1-2: Flow Chart for Piping Stress-Strain Correlation

2.0 PIPING STRAIN CRITERIA

The piping strain criteria proposed for the SONGS-1 LTS are based on the criteria presented in the ASME Code for faulted (Level D) conditions. The piping qualification criteria are based on limiting piping strain levels to ensure that the piping maintains its structural integrity under the earthquake loadings.

The basis of the ASME Code, Section III, Appendix F for faulted conditions [1] is that the piping will remain structurally integral and that the pressure boundary will remain intact. The Code recognizes that the Appendix F rules allow for large deformations of the piping system. The SONGS-1 criteria augments the ASME Code, Appendix F, criteria because the SONGS-1 limits also ensure piping integrity. "Piping integrity" is defined herein as piping which maintains structural integrity and shows no significant decrease in rated flow capacity.

Piping integrity can be defined by the establishment of limits on material strains to ensure the limitation of deformation and to provide a suitable margin to rupture. The strain limits established for the LTS piping evaluation are:

$\epsilon_t \leq 1\%$ for carbon steel
$\leq 2\%$ for stainless steel

where

ϵ_t = Maximum piping membrane plus bending strain

In cases where the strain for stainless steel exceeds 1%, the effects on the following items will be reviewed:

- Plastic tensile instability (tensile necking)
- Low-cycle fatigue (5 full cycles or less)
- Compressive wrinkling (local buckling)
- Excessive deformation resulting in more than a 15% reduction in pipe cross-section flow area
- Pipe-mounted equipment qualification

Justifications of the above strain limits were presented in an earlier submittal to the NRC [5]. A detailed discussion of application limitations for stainless steel strain exceeding 1% is presented in Section 5.0.

3.0 STRESS-STRAIN CORRELATION METHODOLOGY

To calculate the piping strains up to the limits specified in Section 2.0 requires inelastic or nonlinear analysis methods. However, the performance of nonlinear analysis is expensive and time-consuming. Therefore, an approach which allows the use of standard linear elastic analysis techniques and conservatively converts the elastically-calculated stresses to strains is desirable. The evaluation methodology to be used for LTS will provide for standard piping evaluations, but will correlate conservatively with the specified strain limits. The proposed conversion is as follows:

For carbon steel: $$\epsilon_t = K_S \frac{\sigma_e}{E}$$

For stainless steel: $$\epsilon_t = K_S \frac{2.0\,\sigma_e}{E}$$

where

ϵ_t = Maximum piping membrane plus bending strain

σ_e = Elastically-calculated stress for pressure, gravity and seismic loadings, based on stress intensification factor approach, psi (See Section 1.0 for definition)

E = Young's modulus, psi (obtain E from Appendix I of the Code [1])

K_S = Strain correlation factor.

The factor of 2.0 multiplied to $K_S\,\sigma_e/E$ for stainless steel material is an empirically determined value, as descussed in Section 4.2.

The strain correlation factor K_S is defined as follows:

$K_S = 1.0$ When $3.4 \frac{\sigma_e}{S_y} \leq 1.0$

$K_S = 1.0 + \frac{1 - n}{n(m-1)} \left(3.4 \frac{\sigma_e}{Sy} - 1\right)$ When $1.0 < 3.4 \frac{\sigma_e}{S_y} \leq m$

$K_S = 1/n$ When $m < 3.4 \frac{\sigma_e}{S_y}$

where

S_y = Piping material yield strength at maximum operating temperature, psi (obtain S_y from Appendix I of the Code [1]).

n = Strain hardening exponent

m = Code-defined parameter to produce correct correlation

The material parameters n and m used on SONGS-1 piping are defined in Table NB-3228.3(b)-1 of the Code [1] and are summarized below:

Material	m	n
Stainless Steel	1.7	0.3
Carbon Steel	3.0	0.2

4.0 JUSTIFICATION OF METHODOLOGY

The stress-strain correlation methodology is based on the fatigue evaluation procedure of the ASME Code [1] and is verified by comparison with test results, particularly the Greenstreet elbow test results [6]. Both bases are described below.

4.1 ASME Code Fatigue Evaluation Procedure

As discussed in Section 3.0, several approaches have been identified to determine strains in piping systems from elastically-calculated stresses. Based on a review of the alternatives, the approach selected is based on the fatigue evaluation procedures of the ASME Code [1]. This approach is chosen because the ASME Code fatigue evaluation is a strain-based methodology (i.e., the Code design fatigue curves are developed from strain-controlled fatigue data and are converted to representative stresses which are not the actual stresses applied but have the advantage of being directly comparable to stresses calculated on the assumption of elastic behavior). Also, the Code fatigue evaluation contains a procedure for the simplified elastic-plastic evaluation of piping components. By reviewing the background behind these procedures, it is concluded that this philosophy and approach provides a method for conservatively calculating strains from elastically-calculated stresses.

The ASME Code simplified elastic-plastic methodology was developed to account for the effects of the strain concentration phenomenon which occurs when stresses are greater than the yield stress. This is shown in Figure 4-1. When the stress exceeds the yield stress, the actual strain, ϵ_t, exceeds the elastically-calculated strain, ϵ_e, which is simply the elastically-calculated stress divided by the Young's modulus (σ_e/E). The Code defines the strain concentration factor, K_e, to measure the differences between the elastically-calculated strain and the actual strain beyond the yield point. As shown from Figure 4-2a, the strain concentration factor is constant and equal to elastic stress concentration factor between Points A and B, when the material behavior is perfectly elastic. The strain concentration factor increases steadily above yield stresses until a maximum value is reached (Point C in Figure 4-2a). The strain concentration decreases after this as the deflection increases.

The Code idealizes the above material behavior by introducing the strain concentration factor Ke and approximates the strain concentration factor by the following formula:

$$K_e = 1.0 \qquad \text{when } S_n \leq 3Sm \text{ (or } 2\ Sy)$$

$$K_e = 1.0 + \frac{1 - n}{n(m-1)} \left(\frac{Sn}{3Sm} - 1\right) \qquad \text{When } 3Sm < S_n \leq 3\ m\ S_m$$

$$K_e = 1/n \qquad \text{when } 3m\ S_m < S_n$$

where

Sn = Primary plus secondary stress intensity range, psi, as calculated in NB-3653.1 of the Code [1]

Sm = Allowable design stress intensity value at maximum operating temperature, psi (obtain Sm from Appendix I of the Code [1]).

Sy, m and n = As defined in Section 3.0.

The terms m and n are material properties developed from experimental data. As shown from Figure 4-2b, the maximum strain concentration is defined by the inverse of the material parameter n and the slope of the strain concentration in the transition region (between 1.0 and 1/n) is defined by $(1-n)/n(m-1)$. Figure 4-3 shows the relationship between the strain concentration and stress for the Code and several tests on 304 Stainless Steel.

The K_e factor developed for the Code fatigue evaluation correlates the elastically-calculated stresses to actual strains for use in the Code fatigue curves. For the SONGS-1 Seismic Reevaluation Program, the K_e methodology will be used to determine strains in the piping associated with the seismic loading.

The strain correlation developed by the Code is modified slightly herein to account for the half-range stresses calculated by the Class 2 Code approach for the SONGS-1 LTS evaluation. The term 3.4 σ_e/Sy of the strain correlation factor K_S for SONGS-1 is equivalent to Sn/3Sm of the strain concentration factor Ke in the Code. A factor of 3.4 is derived as follows:

- The ratio of full range stresses vs. one-half range stresses is 2.0
- The Class 1 stress index C_2 vs. the Class 2 stress intensification factor 0.75i for butt-welded elbow* is:

$$\frac{C_2}{0.75i} = \frac{1.95/h^{2/3}}{0.75 \times 0.9/h^{2/3}} = 2.9$$

where

h = Elbow flexibility factor, as defined in NB-3683.7 of the Code [1] (Same as Class 2).

- minimum ratio of material allowable 3Sm/Sy is 1.71 for carbon steel A-106 Grade B at room temperature.

Note * Elbows are of particular importance because they are often the most flexible components in a piping system. Elbows are forced to accommodate disproportionate displacements arising from various loadings including earthquake. Therefore, in general, the integrity of elbows will govern the integrity of a piping system.

Therefore, $\frac{S_n}{3S_m} = \frac{2.9 \times 2.0}{1.71} \times \frac{\sigma_e}{S_y} = 3.4 \frac{\sigma_e}{S_y}$

4.2 Comparison with Greenstreet Elbow Test Results

Description of Tests

The experimental work performed by Greenstreet [6] determined load-deflection and load-strain responses for sixteen 6-inch (nominal) commercial carbon steel pipe elbows and four 6-inch stainless steel elbows. The material for carbon steel elbows is ASTM A-106, Grade B and the material for stainless steel elbows is ASTM A-312, Type 304L. These material properties closely match with those used on SONGS-1 piping. Each specimen was loaded with an external static force of sufficient magnitude to produce predominantly plastic response. The influences of elbow bend radius (long radius and short radius) and wall thickness (Sch. 40 and Sch. 80), as well as the effect of internal pressure (five specimens were loaded with internal pressure) were studied. The load-deflection curves and load-strain curves obtained in the tests were limited by the test apparatus. As a result, the test results used in the comparison do not represent the maximum capacity of the elbows.

Greenstreet plotted ten load-strain curves, all without internal pressure. A detailed breakdown of these tests is summarized below:

Figure Number					Loading Condition	
For This Report	For Greenstreet Report	Specimens	Descrip.	Material(2)	Moment(1)	Pressure
A-1	22	PE-1	Sch.40-LR	C.S.	in-plane(+)	No
A-2	23	PE-2	Sch.40-LR	C.S	in-plane(-)	No
A-3	24	PE-3	Sch.40-LR	C.S.	out-of-plane	No
A-4	25	PE-8	Sch.80-LR	C.S.	in-plane(-)	No
A-5	26	PE-11	Sch.40-SR	C.S.	in-plane(-)	No
A-6	33	PE-19	Sch.40-SR	C.S.	in-plane(-)	No
A-7	34	PE-20	Sch.80-SR	C.S.	in-plane(-)	No
A-8	27	PE-15	Sch.40-LR	S.S.	in-plane(-)	No
A-9	31	PE-17	Sch.40-SR	S.S.	in-plane(-)	No
A-10	32	PE-18	Sch.80-LR	S.S.	in-plane(-)	No

Note: (1) A positive in-plane moment causes the elbow to open; a negative in-plane moment causes the elbow to close.

(2) C.S.: Carbon Steel ASTM A-106, Grade B
S.S.: Stainless Steel ASTM A-312, Type 304L.

Intepretation of Comparison

Appendix A shows load-strain curves reported by Greenstreet together with load-strain curves calculated by SONGS-1 stress-strain correlation methodology. A factor of 2.0 is multiplied to $K_S \sigma_e/E$ for stainless steel material in order to conservatively derive a satisfactory comparison with test results. In reviewing these load-strain curves, the following observations are made:

1. The SONGS-1 stress-strain correlation methodology will overpredict the strains, when compared with the Greenstreet test results. The overprediction is in the range of 25 percent to 100 percent for nine out of ten load-strain curves (excluding specimen PE-19).

2. For specimen PE-19, test-recorded strains are approximately 10 percent higher than the calculated strains in the vicinity of the test cut-off region.

3. With extrapolation, it appears that the calculated strains and test-recorded strains will converge at higher strain levels.

The 10 percent exceedance for specimen PE-19 (observation 2) and the potential convergence at higher strain levels for other specimens (observation 3) are not a concern because of the very conservative comparison made. Major conservatisms in the comparison are discussed as follows:

- The calculated strains based on SONGS-1 stress-strain correlation methodology are intended to predict membrane-plus-bending strains, i.e. strain averaged through the wall thickness plus strains at the surface due to an equivalent linear distribution of strain through the wall thickness. As stated in the Greenstreet test report [6], the test load-strain curves were plotted for locations with strain gages mounted at or near the "maximum" or "principal" strains on elbow surfaces.

  Figure 4-4 shows an elbow crotch section under in-plane bending. In-plane bending was applied to all tests with load-strain curves plotted, except PE-3. Strain gages at 90°, 270° and the near vicinity (0° is at extrados and 180° at intrados) would pick up predominent circumferential strains because the axis crossing 90° and 270° is a major axis of ovality for the deformed cross section, as well as a neutral axis under in-plane bending. Strain gages at 0°, 180° and the near vicinity would pick up both axial and circumferential strains, with the axial strain at its maximum. Figure 4-5 shows the maximum axial and the maximum circumferential strain distribution through the wall thickness under in-plane bending. The axial strain is more or less linearly distributed through the wall thickness and is therefore a membrane-plus-bending type strain. However, the circumferential strain contains local or peak effect (local strains at any point). This is particularly evident for the elbow's inside surface at or near the major axis of

the crotch section. Greenstreet plotted the circumferential strain versus angular location (from 0° to 180°) as function of load for specimens PE-18 and PE-19 (Figures 29 and 30 in [6]). Near the 90° location, where the maximum circumferential strain appears, the test-recorded strain on the inside surface is much higher than the test-recorded strain on the outside surface. Since the tests were performed without internal pressure, the membrane part of the circumferential strain should be small. This indicates that the test-recorded circumferential strain is not linearly distributed through the wall thickness and therefore contains local or peak effects, particularly on the inside surface.

A review of the Greenstreet test load-strain curves indicates that the gage locations for the maximum strains are, for most cases, at or near 90° and 270°. For Specimen PE-19, the load-strain curve was plotted for the maximum strains located on inside surface at the 90° location (strain gage number A+2 as shown in Figure 4-4). At this location, the local strain effect is at its maximum.

As a conclusion, it is conservative to compare the calculated membrane-plus-bending strains with test-recorded maximum strains which contain local or peak effect.

- All load-strain curves reported by Greenstreet are from tests where the elbows were not pressurized. In actual cases, elbows are typically pressurized and the internal pressure will improve the integrity and stability of elbows. This is because by reducing the elbow flexibility with its internal pressure, the measured strains, both the axial and the circumferential, would be reduced.

- The test load-strain curves beyond the test cut-off points were extrapolated by straight lines which are tangent to the test cut-off regions as shown by dotted lines on several load-strain curves. These extrapolated straight lines are relatively flat. In actual cases, the test load-strain curves should be skewed upward beyond the test cut-off points due to the strain hardening phenomenon.

- The loads in the Greenstreet tests were applied statically. Studies [7] show that the margin against failure of piping systems is significantly greater for dynamic loads, such as an earthquake, than for static loads when piping responses are held to the same allowable level. Also, in establishing the allowable strains for SONGS-1, the material overstrength and strain rate effects under dynamic loads were not credited.

Conclusion

The calculated strains based on SONGS-1 stress-strain correlation methodology are conservative, when compared with experimentally determined strains.

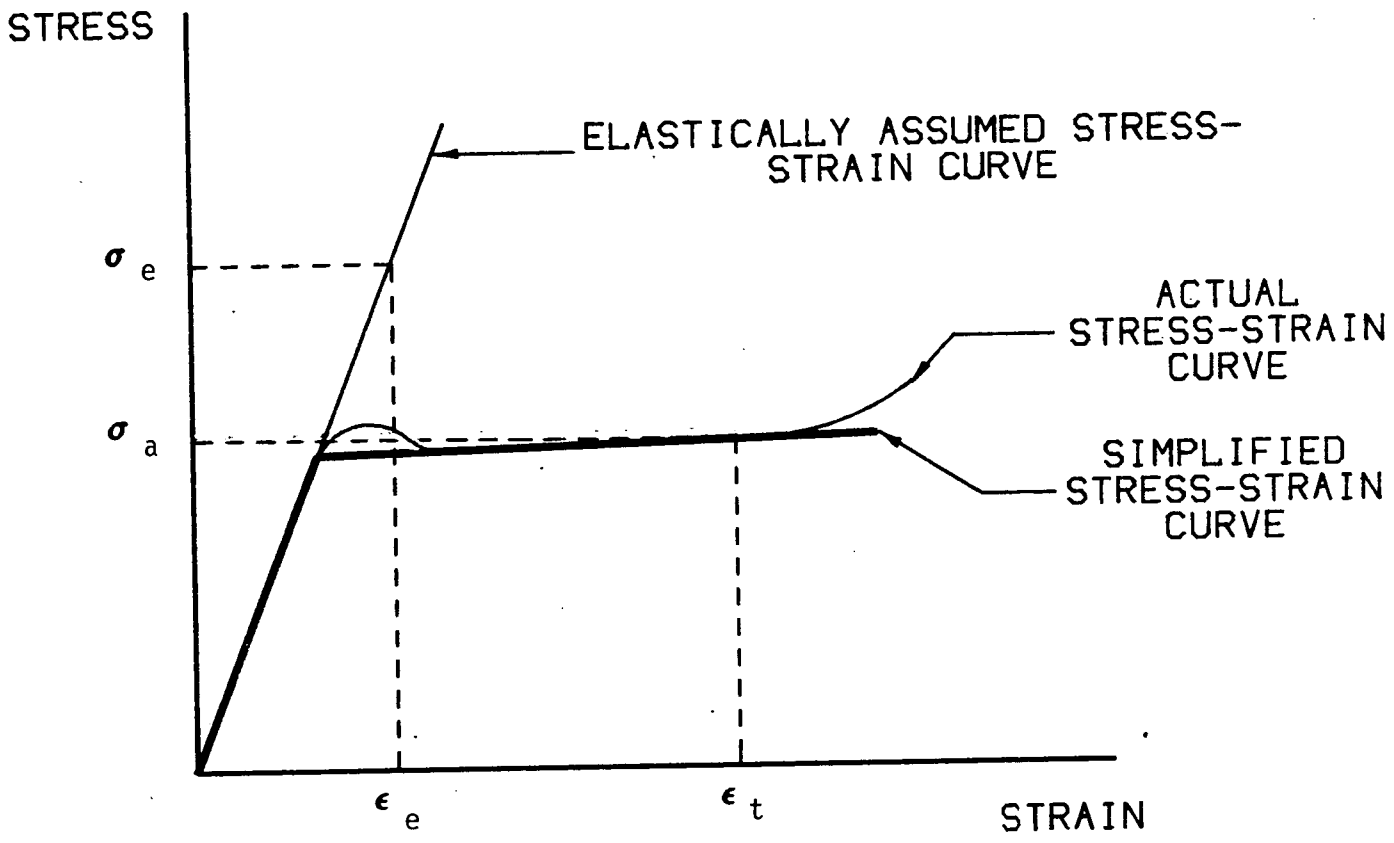

σ_e = ELASTICALLY CALCULATED STRESS

ϵ_e = ELASTICALLY CALCULATED STRAIN ($\epsilon_e = \sigma_{e/E}$)

ϵ_t = TOTAL OR ACTUAL STRAIN

σ_a = ACTUAL STRESS

FIGURE 4-1
ELASTIC STRAIN VS. ACTUAL STRAIN

a. Actual Case

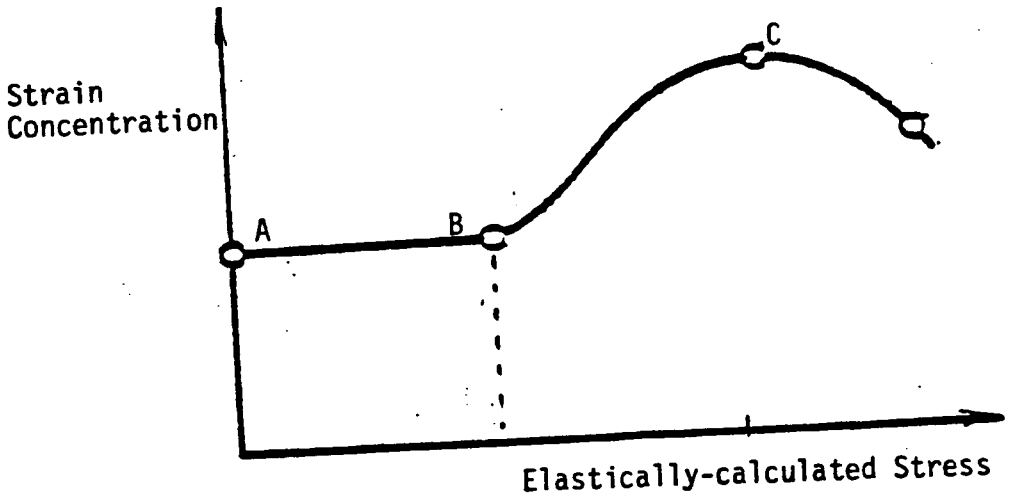

b. Code Idealized Approach

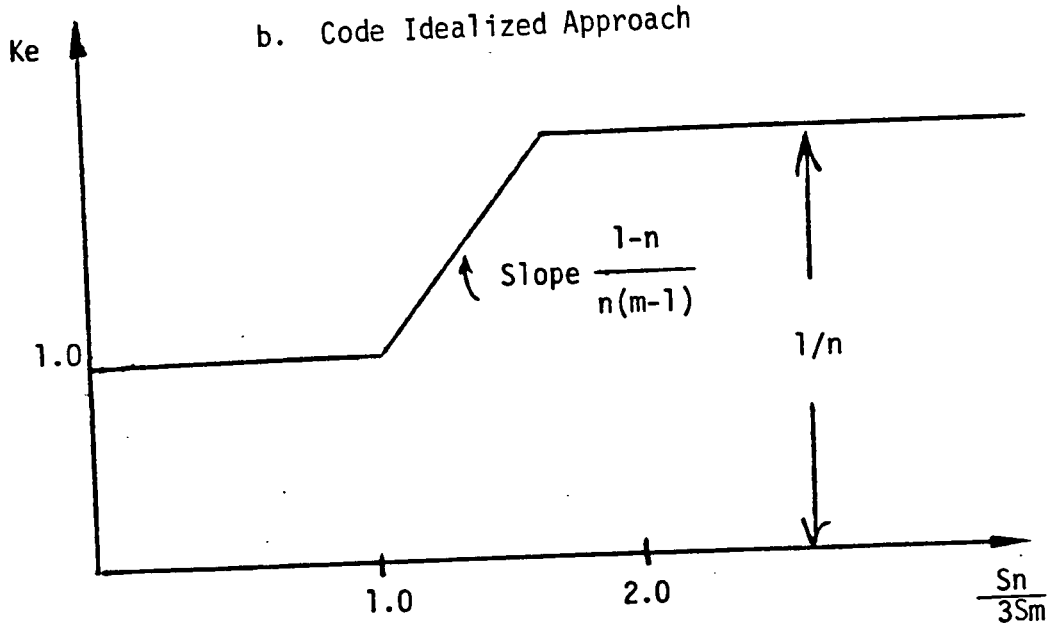

FIGURE 4-2 CODE STRAIN VS. STRESS RELATION

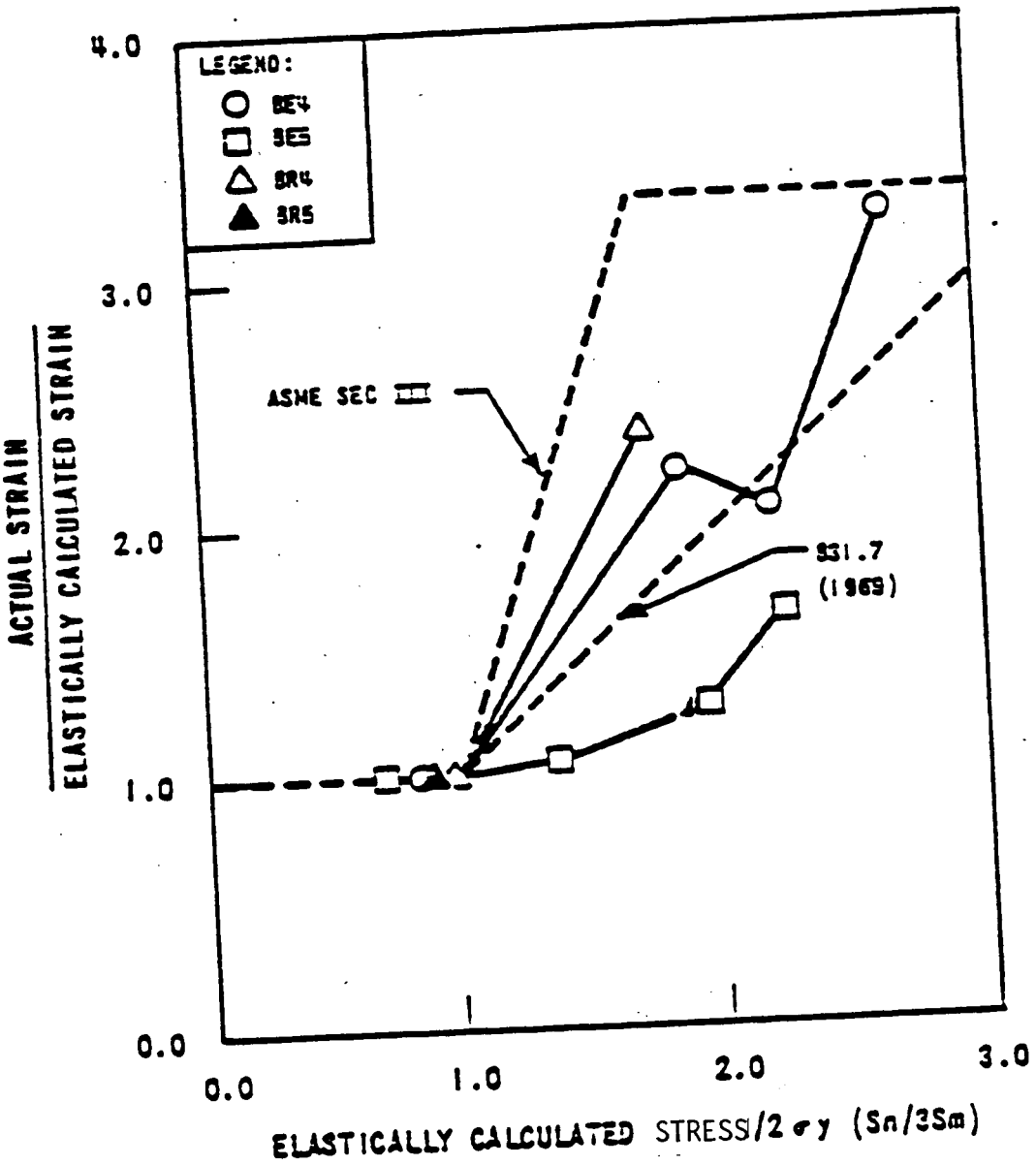

FIGURE 4-3 CODE VS. TEST STRAIN-STRESS RELATION

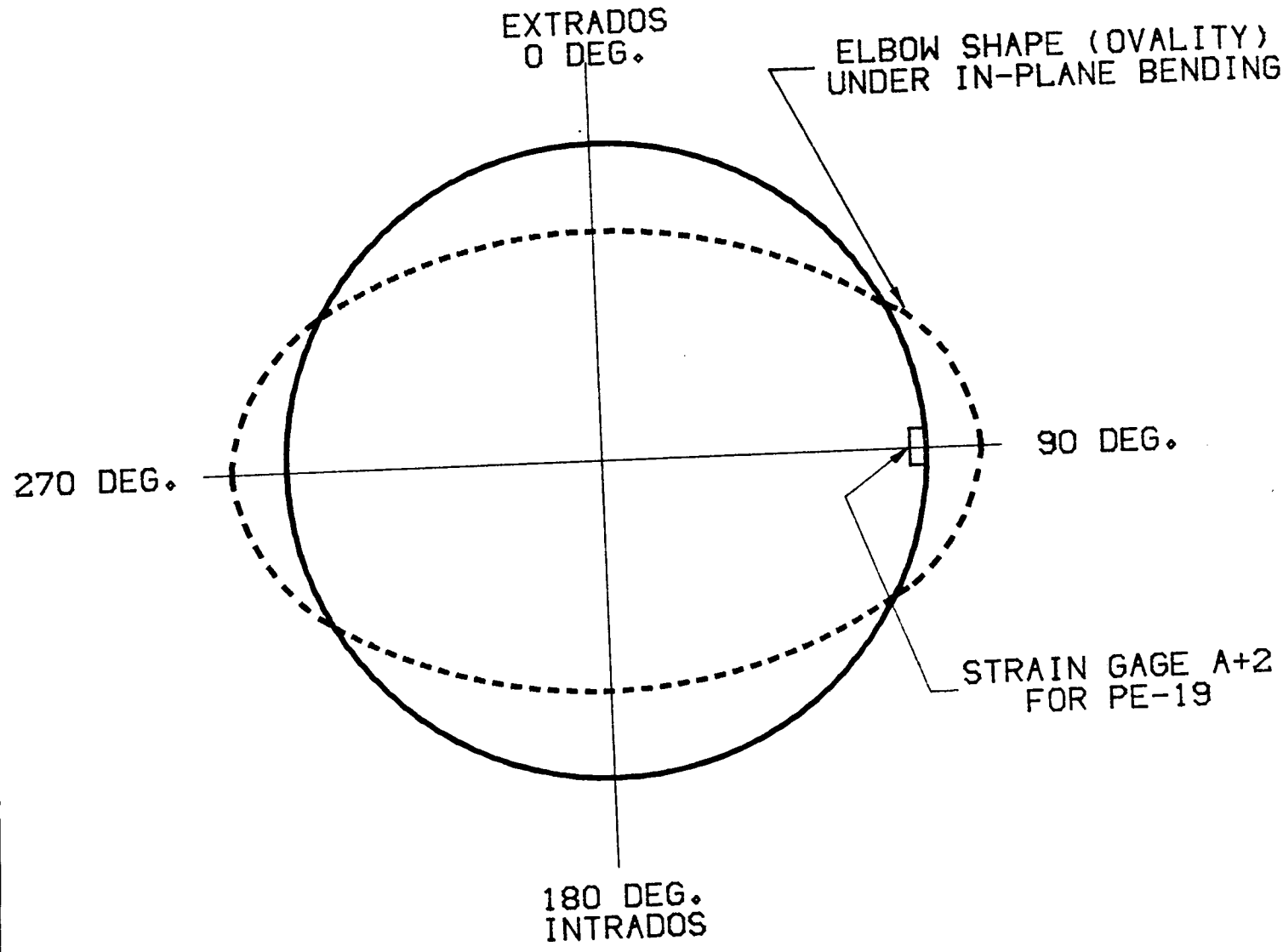

FIGURE 4-4
ELBOW CROTCH SECTION
UNDER IN-PLANE BENDING

MAX. AXIAL STRAIN
AT 0° OR 180°

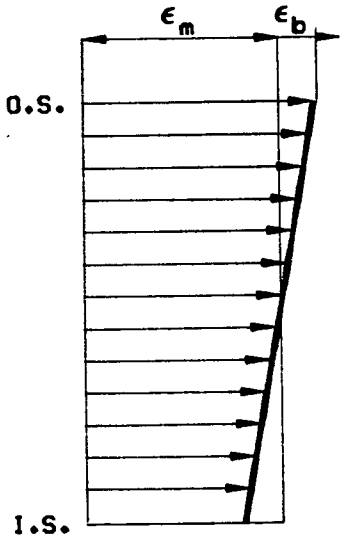

MAX. CIRCUMFERENTIAL
STRAIN AT 90° OR 270°

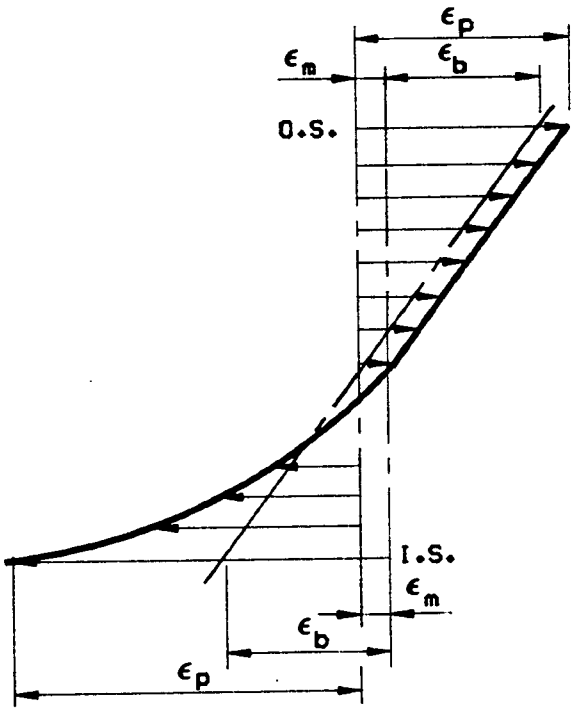

LEGEND: ϵ_m - MEMBRANE STRAIN
ϵ_b - BENDING STRAIN
ϵ_p - LOCAL OR PEAK STRAIN
O.S. - OUTSIDE SURFACE
I.S. - INSIDE SURFACE

FIGURE 4-5

MAXIMUM STRAIN DISTRIBUTION THROUGH THE WALL THICKNESS UNDER INPLANE BENDING

5.0 APPLICATION LIMITATIONS

For stainless steel piping, additional checks will be performed if the calculated strains using the stress-strain correlation methodology exceed 1 percent, but no more than 2 percent. The five concerning items as discussed in Section 2.0 will be reviewed as follows:

- For tensile plastic instability, low-cycle fatigue and compressive wrinkling concerns, either one of the following two checks will be performed:

Option 1:

$$\epsilon_t \leq 0.2 \frac{t}{R}$$

where

ϵ_t = Strain as calculated in Section 3.0
t = Nominal wall thickness of pipe, in
R = Mean radius of pipe, in

Option 2:

$$\frac{n}{N} \leq Ua$$

where

n = Number of significant cycles for Modified Housner Earthquake
N = Number of allowable cycles for Modified Housner Earthquake
Ua = Allowable usage factor for Modified Housner Earthquake

N will be calculated as follows:

$$N = \left[\frac{91.875}{0.75i \frac{M}{Z}}\right]^5$$

where

i and z = As defined in Section 1.0

M = Resultant elastically-calculated moment due to Modified Housner Earthquake inertia and anchor movements. The inertia moment may be combined with the seismic anchor movement moment by SRSS method.

For Option 2, the number of significant cycles for Modified Housner Earthquake (n) will be assumed to be 5. This value was recommended as a realistic estimate in [8]. The allowable usage factor for Modified Housner Earthquake (Ua) will be assessed on a case-by-case basis, depending on the operating conditions of a particular piping

system under review. The value of Ua is highly dependent on the cumulative usage factor from other cyclic loadings, i.e., thermal expansion cycling in conjunction with thermal transient cycling and other dynamic load cycling.

- For the excessive deformation concern, studies [9] show that at the maximum 2 percent strain level for stainless steel, the maximum ovalization and flow rate reductions were considered to be acceptable (less than 5 percent flow area reduction). For the Greenstreet tests [6], the maximum strain level as limited by the test apparatus (less than 1 percent) would produce a maximum ovality of 9 to 15 percent. A 15 percent ovality corresponds to less than 1 percent of flow area reduction. These studies and tests indicate that at 2 percent strain level for stainless stress elbows, the flow area reduction would be much less than the 15 percent flow area reduction (recommended as a flow area reduction limit in [8]). Therefore, the excessive deformation check is readily satisfied.

- For the pipe-mounted equipment qualification, all nozzle loads and mechanical equipment in the LTS scope will be qualified to the Code allowables, regardless of whether the connecting pipe is qualified by the SEP guidelines or by the stress-strain correlation approach [2,3,4].

In addition, all piping qualification calculations will be identified to the NRC for review on a case-by-case basis where calculated strains for stainless steel exceed 1 percent and/or deviations from the stated stress-strain correlation methodology are applied.

REFERENCES

1. ASME B&PV Code, Section III, 1980 Edition with Addenda through Winter 1980.

2. SCE Document "SONGS-1 Seismic Program for LTS", Submitted to the NRC on March 8, 1985.

3. SCE Document "SONGS-1 LTS Seismic Reevaluation Program, Status Report for All Action Items Identified from the NRC Letter dated March 27, 1985", Submitted to the NRC on May 31, 1985.

4. NRC's Safety Evaluation Report "LTS Plan - SEP Seismic Reevaluation Criteria and Methodology, SONGS-1", Docket No. 50-206, dated September 1985.

5. SCE Document "SONGS-1 LTS Seismic Reevaluation Program, Technical Basis for Piping Strain Limits and Development of Linear, Elastic Analysis Methodology," Submitted to the NRC on May 31, 1985.

6. Greenstreet, W.L., "Experimental Study of Plastic Response of Pipe Elbows," ORNL/NUREG 24, February 1978.

7. Campbell, R.D., et. al., "Development of Dynamic Stress Criteria for Design of Nuclear Piping Systems," Structural Mechanics Associates Inc. Report No. 17401-01, Prepared for Pressure Vessel Research Committee, November 1982.

8. NUREG 1061, Volumes 2, "Report of the U.S. Nuclear Regulatory Commission Piping Review Committee, Evaluation of Seismic Designs - A Review of Seismic Design Requirements for Nuclear Power Piping", April 1985.

9. Impell Report No. 04-0310-0063, "SONGS-1 Functionality Criteria for Piping Systems in Response to the DBE Event," Revision 2, December 1983 (Transmitted to the NRC in SCE Letter to NRC, from K. Baskin to D.M. Crutchfield dated December 23, 1983).

APPENDIX A: Comparison of Load-Strain Curves Between Greenstreet Tests and SONGS-1 Stress-Strain Correlation Methodology

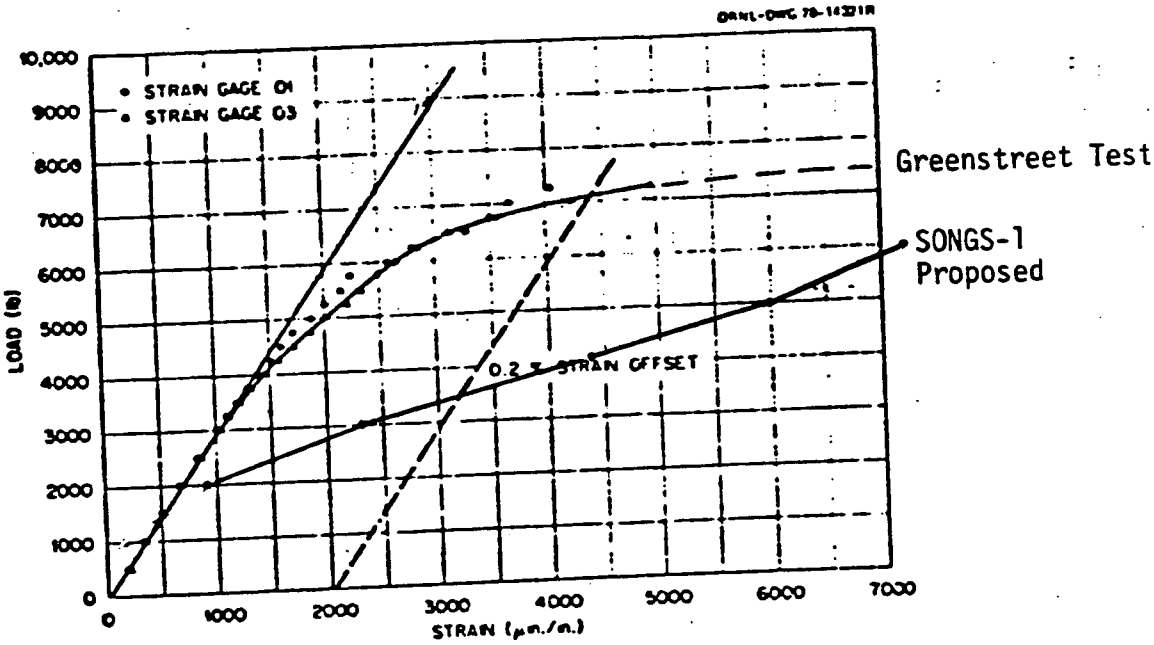

Fig. 22. Load-strain data for in-plane bending ($+M_z$) of specimen PE-1 (1 lb_f = 4.448 N).

FIGURE A-1

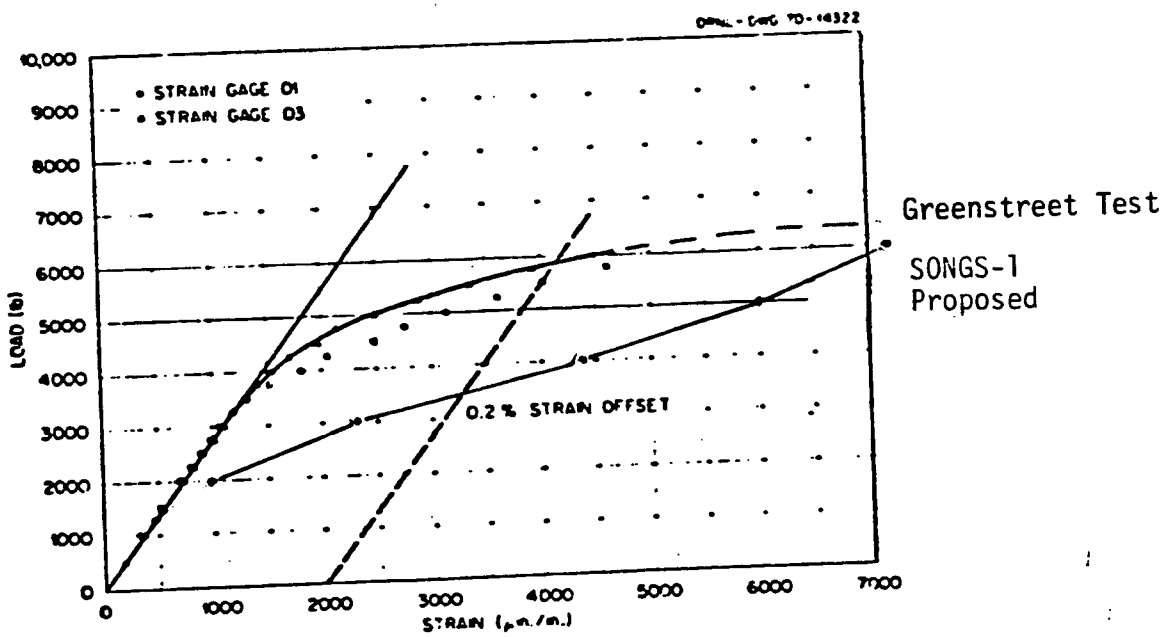

Fig. 23. Load-strain data for in-plane bending ($-M_z$) of specimen PE-2 (1 lb_f = 4.448 N).

FIGURE A-2

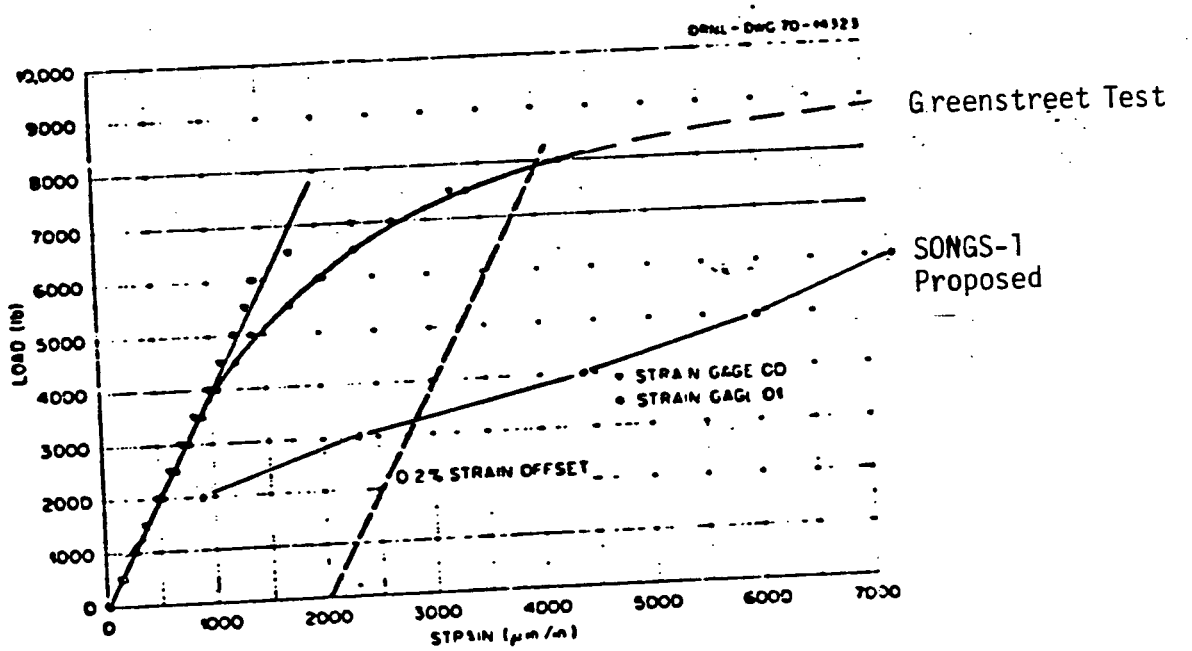

Fig. 24. Load-strain data for out-of-plane bending (M_y) of specimen PE-3 (1 lb_f = 4.448 N).

FIGURE A-3

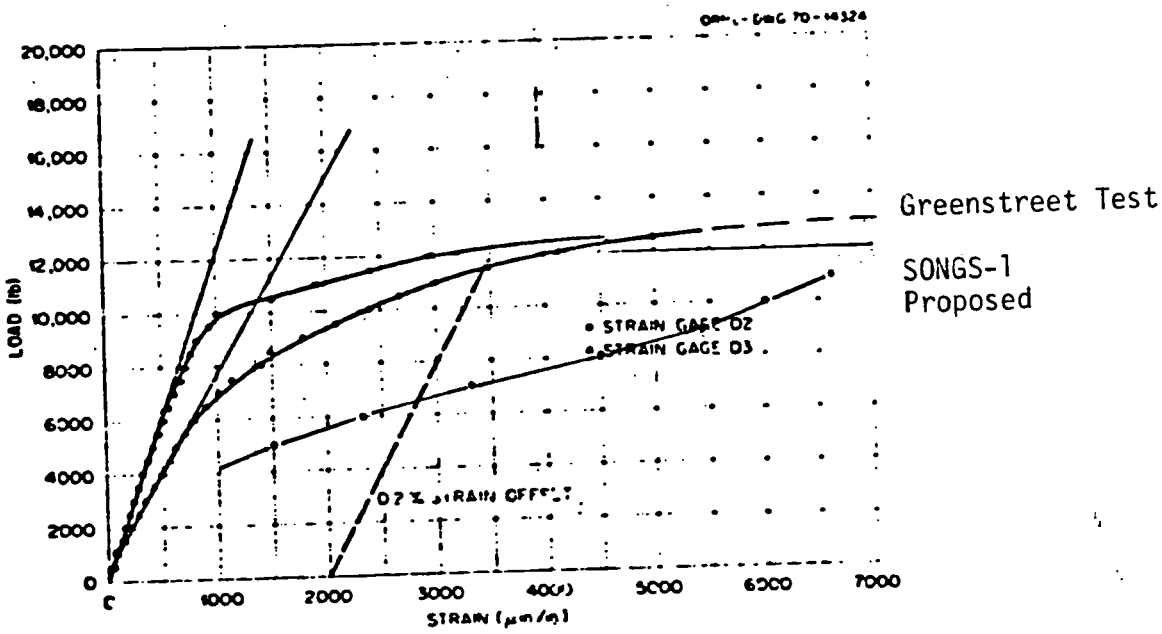

Fig. 25. Load-strain data for in-plane bending ($-M_z$) of specimen PE-8 (1 lb_f = 4.448 N).

FIGURE A-4

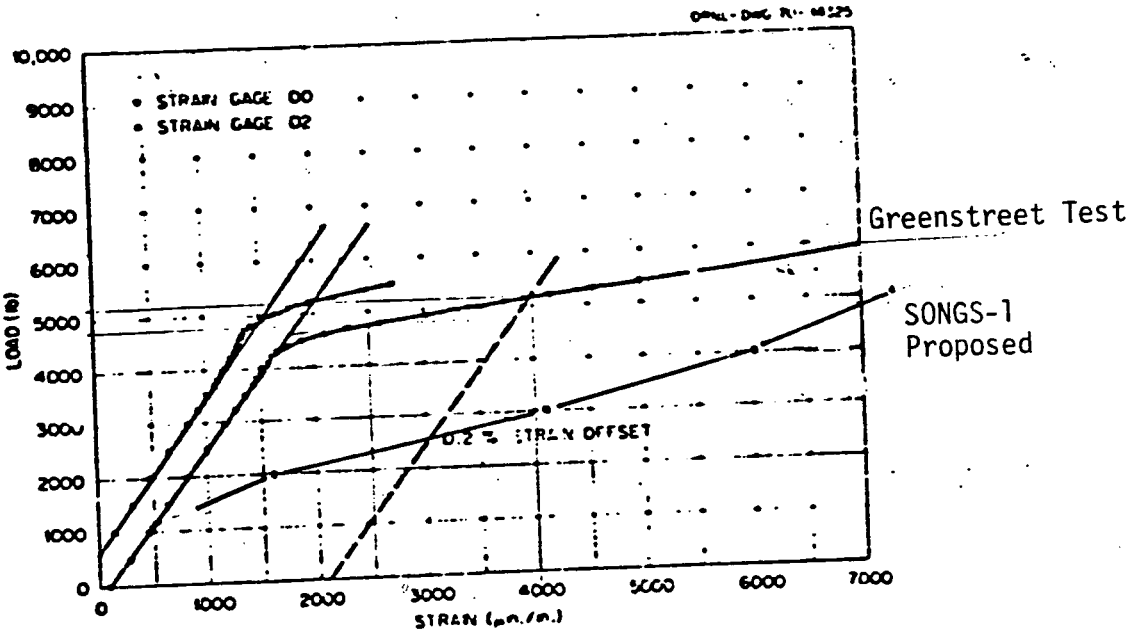

Fig. 26. Load-strain data for in-plane bending ($-M_z$) of specimen PE-11 (1 lb_f = 4.448 N).

FIGURE A-5

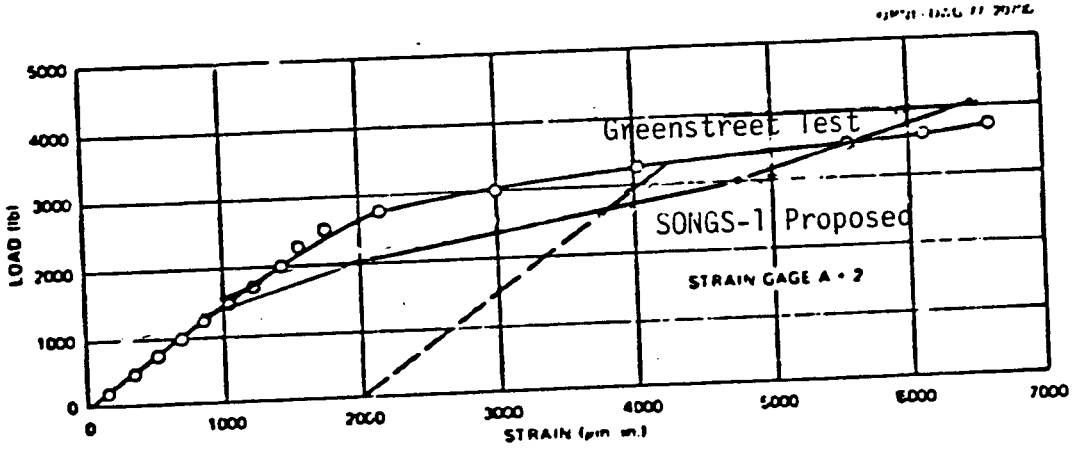

Fig. 33. Load-strain data for in-plane bending ($-M_z$) of specimen PE-19 (1 in. = 25.4 mm; 1 lb_f = 4.448 N).

FIGURE A-6

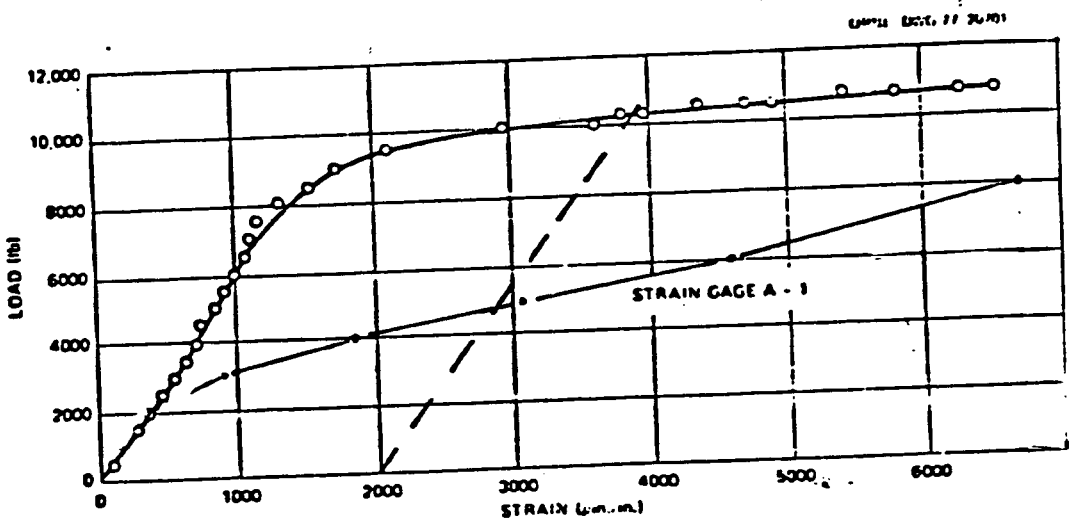

Fig. 34. Load-strain data for in-plane bending ($-M_z$) of specimen PE-20 (1 in. = 25.4 mm; 1 lb_f = 4.448 N).

FIGURE A-7

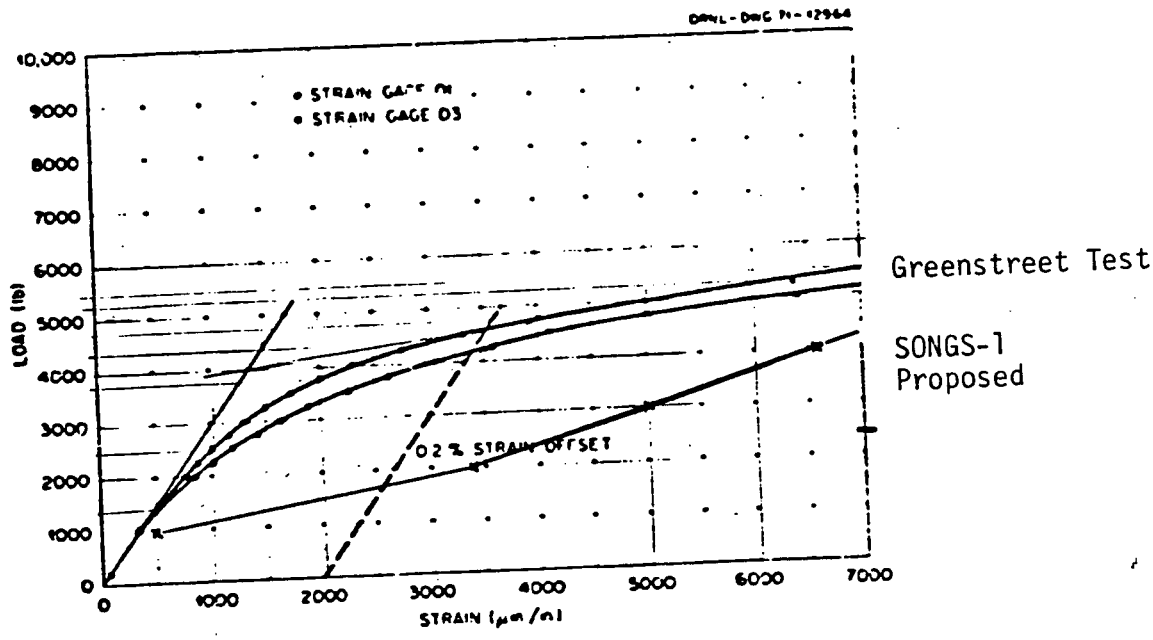

Fig. 27. Load-strain data for in-plane bending ($-M_z$) of specimen PE-15 (1 lb_f = 4.448 N).

FIGURE A-8

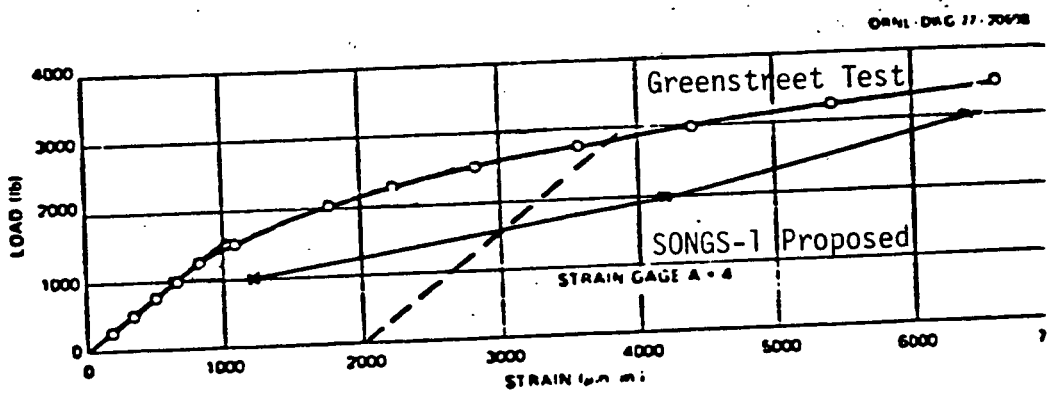

Fig. 31. Load-strain data for in-plane bending ($-M_z$) of specimen PE-17 (1 in. = 25.4 mm; 1 lb_f = 4.448 N).

FIGURE A-9

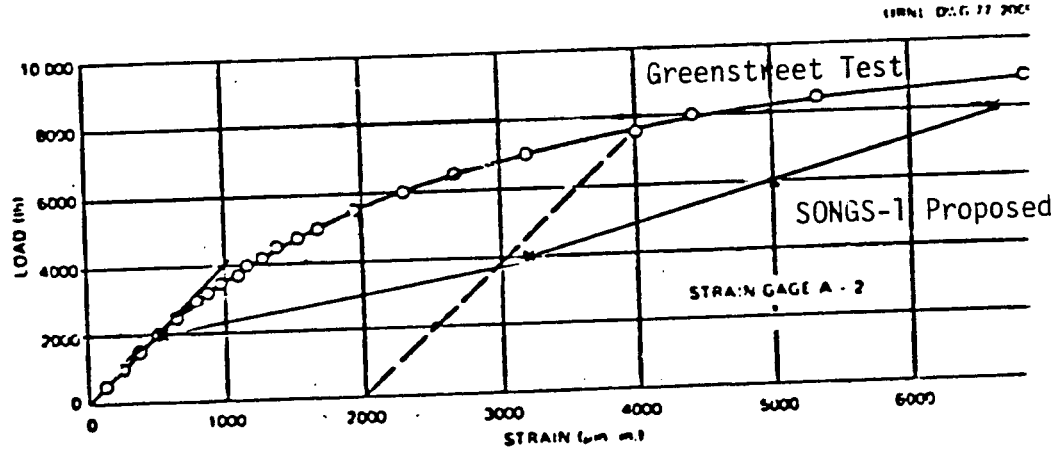

Fig. 32. Load-strain data for in-plane bending ($-M_z$) of specimen PE-18 (1 in. = 25.4 mm; 1 lb_f = 4.448 N).

FIGURE A-10